U. S. DEPARTMENT OF COMMERCE NATIONAL BUREAU OF STANDARDS

RESEARCH PAPER RP1138

Part of Journal of Research of the National Bureau of Standards, Volume 21, October 1938

MEASUREMENT OF RELATIVE AND TRUE POWER FACTORS OF AIR CAPACITORS[1]

By Allen V. Astin

ABSTRACT

An alternating-current bridge for measuring the differences of power factor of capacitors to $\pm 5\times10^{-7}$ in the commercial and audio-frequency range is described. The bridge is essentially of the Schering type, with a Wagner ground connection, and may be arranged for either high- or low-voltage use. The theory of the bridge is given for both perfect and imperfect balance, the latter permitting evaluation of the error due to residual voltages.

Variable low-loss air capacitors for use in the bridge are described. It is shown that the power factor of a guard-ring air capacitor is not necessarily zero, and a method is given for determining the true value of this power factor.

CONTENTS

I. INTRODUCTION

As part of a program for the investigation of electrical-insulation problems, it was found necessary to develop an alternating-current bridge for measuring capacitor power factors of the order of 1×10^{-6}. At the time the work was started (1930) the precision of power-factor bridges, as described in the literature [1, 2],* was of the order of 1×10^{-5}. The precision has been extended to about 1×10^{-6} since that time [3, 4]. Previous methods have been confined primarily to a measurement of the differences in the power factors of capacitors, and there has apparently been no satisfactory procedure for determining the absolute or true values of these power factors. In the present work a method has been developed for evaluating the true

[1] A large part of this work was done by the author as a research associate for the Utilities Research Commission of Illinois in 1930–32. The work completed at that time was summarized at the annual meeting of the Electrical Insulation Committee of the National Research Council in 1932 and an abstract published in Elec. Eng. **52**, 104 (1933).

* Figures in brackets indicate the literature references at the end of this paper.

power factors of low-loss capacitors,[2] and a bridge has been designed for measuring very small differences in their power factors.

All bridges for small power-factor measurements of capacitors are similar in that they are fundamentally Schering [5] bridges, as shown in figure 1. Here the bridge circuit is made up of capacitors and resistors, the phase angles being balanced by the capacitance in parallel with resistance. The various bridges differ in the points of connection for the source and detector and in the methods of grounding and shielding. In the bridges of Kouwenhoven [4] and Balsbaugh [3] the power is applied at the C_1, C_2 junction and the R_3, R_4 junction, as in the original Schering bridge, so that, in general, the bridge offers a high impedance to the source. This high impedance makes the bridge suitable for high-voltage work, and henceforward such an orientation of the source and the detector will be referred to as the high-voltage form of the bridge. In the Ogawa [2] bridge the power is applied in the C_1, R_3 junction and the C_2, R_4 junction, thus presenting a low impedance to the source and a high impedance to the detector. This latter arrangement has recently been called a conjugate Schering bridge [6]. Dye and Jones [7] have used a variation of the conjugate bridge for power-factor measurements of the order of 1×10^{-5} with frequencies up to 1,000 kc/s.

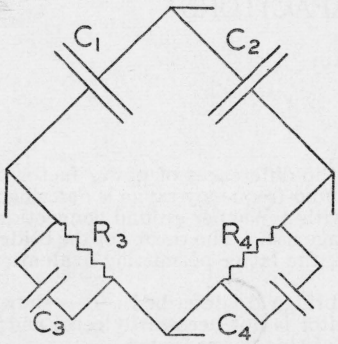

FIGURE 1.—*Arrangement of admittances in a Schering-type bridge.*

In the original, or high-voltage form, power is applied on the horizontal connectors and in the low-voltage, or conjugate form, on the vertical connectors.

The conjugate arrangement of the bridge makes the use of Wagner's [8] grounding method very natural and simplifies the shielding of the parts of the bridge. Ogawa has also pointed out a method of using the Wagner ground with the high-voltage form of the bridge. The bridge forms to be described in this paper are extensions of those of Ogawa. The Schering bridge (fig. 1) forms the bridge proper, grounding is obtained by Wagner's method and a switching arrangement (to be described) permits connecting the bridge for either high- or low-voltage work. In extending the precision beyond that obtained previously, a method of balancing out residual effects due to imperfect wave form and imperfect shielding was necessary. This is described in the section on bridge theory.

The reasons for the superiority of the Schering bridge form for small power-factor measurements have been discussed in detail by others, especially Ogawa. They are, however, briefly these: First, the bridge elements are easily shielded since no inductors are present. Second, the absence of series connections in any bridge arm between capacitance and resistance simplifies both the shielding and the evaluation of distributed effects. Third, the bridge balance can be obtained by the adjustment of capacitors only, thus eliminating the effects of changes in the phase angles of the resistors.

[2] This method was described by the author at the annual meeting of the Electrical Insulation Committee of the National Research Council, November 5, 1936, at Boston, Mass. At the 1937 meeting of this committee and at the June 1938 meeting of the AIEE, W. B. Kouwenhoven and E. L. Lotz have described a similar method for determining absolute power factor.

In order to measure small power factors it is necessary that the capacitors, C_1 and C_2 have small power factors. If a bridge is used in which the detector is not brought to ground potential at the balance, a shielding circuit at the detector potential is necessary in addition to ground-potential shields. Thus, if it is desired to use shielded guard-ring capacitors for C_1 and C_2, these capacitors must have four electrodes [3] (two measuring electrodes, one shield-circuit electrode, and one grounded electrode). The use of the Wagner ground brings the detector to ground potential at balance, eliminates the extra shield circuit, and permits the use of three-electrode capacitors for C_1 and C_2 when shielded guard-ring capacitors are necessary. The variable three-electrode capacitors which have been built for use in the bridge will be described later, as well as the method which has been developed for evaluating their power factors.

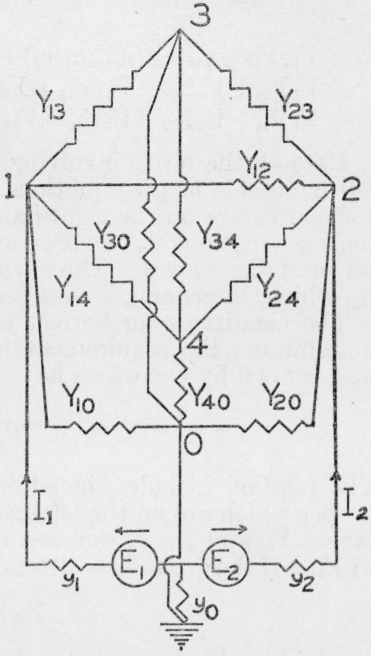

FIGURE 2.—*Location of equivalent stray and ground admittances in a bridge network.*

II. THEORY OF THE BRIDGE

I. LOW-VOLTAGE, OR CONJUGATE SCHERING BRIDGE

(a) PERFECT BALANCE

The general equivalent network arrangement of a bridge with a Wagner ground is shown in figure 2, where 1 and 2 represent the power terminals, 3 and 4 the detector terminals, 0 the ground point, and the Y terms the admittances between the various terminals. The currents from the source to bridge terminals 1 and 2 are I_1 and I_2, respectively.

Following the method of Ogawa, the sum of the currents entering each terminal is equated to zero, giving the following set of equations:

$$\left.\begin{aligned} Y_{12}(V_1-V_2)+Y_{13}(V_1-V_3)+Y_{14}(V_1-V_4)+Y_{10}V_1&=I_1\\ Y_{12}(V_2-V_1)+Y_{23}(V_2-V_3)+Y_{24}(V_2-V_4)+Y_{20}V_2&=I_2\\ Y_{13}(V_3-V_1)+Y_{23}(V_3-V_2)+Y_{34}(V_3-V_4)+Y_{30}V_3&=0\\ Y_{14}(V_4-V_1)+Y_{24}(V_4-V_2)+Y_{34}(V_4-V_3)+Y_{40}V_4&=0 \end{aligned}\right\} \quad (1)$$

where V_1, V_2, V_3, and V_4 are the potentials with respect to ground of terminals 1, 2, 3, and 4. Currents I_1 and I_2 are obtained from the equations:

$$V_1=E_1-I_1/y_1-(I_1+I_2)/y_0 \text{ and } V_2=E_2-I_2/y_2-(I_1+I_2)/y_0 \quad (2)$$

and are

$$\left.\begin{aligned} I_1&=(y_0+y_1)E_1-y_0E_2-(y_0+y_1)V_1+y_0V_2\\ I_2&=(y_0+y_2)E_2-y_0E_1-(y_0+y_2)V_2+y_0V_1 \end{aligned}\right\} \quad (3)$$

Here E_1 and E_2 are the electromotive forces, and y_0, y_1, and y_2 the admittances of a general type of source, which can be represented as shown in figure 2. Upon substituting the values for I_1 and I_2 in eqs 1, and retaining the last two equations of the group and forming two new equations from the difference of the first two and the sum of all four, the following set is obtained:

$$\left.\begin{aligned} &V_1(2Y_{12}+Y_{13}+Y_{14}+Y_{10}+2y_0+y_1)-V_2(2Y_{12}+Y_{23}+Y_{24}+Y_{20}\\ &\quad +2y_0+y_2)+V_3(Y_{23}-Y_{13})+V_4(Y_{24}-Y_{14})=E_1(2y_0+y_1)\\ &\qquad -E_2(2y_0+y_2)\equiv S_1\\ &V_1(Y_{10}+y_1)+V_2(Y_{20}+y_2)+V_3Y_{30}+V_4Y_{40}=y_1E_1+y_2E_2\equiv S_2\\ &V_1Y_{13}+V_2Y_{23}-V_3(Y_{13}+Y_{23}+Y_{34}+Y_{30})+V_4Y_{34}=0\\ &V_1Y_{14}+V_2Y_{24}+V_3Y_{34}-V_4(Y_{14}+Y_{24}+Y_{34}+Y_{40})=0 \end{aligned}\right\} \quad (4)$$

Here all the terms involving the properties of the bridge are on the left-hand side of the equations, and those involving the properties of the source are on the right-hand side. The major source-term is S_1, representing roughly the product of the electromotive force and admittance of the source. The asymmetry of the source is represented by S_2, which, in general, is very small compared with S_1.

The conditions for perfect balance can be obtained from eq 4 by determining the requirement for V_3 to equal V_4. The solution has been shown by Ogawa to be

$$Y_{13}Y_{24}-Y_{23}Y_{14}=\frac{V_3+V_4}{V_3+V_4-2V_1}(Y_{40}Y_{23}-Y_{30}Y_{24}). \quad (5)$$

The relation includes, in addition to the admittances of the bridge proper which are on the left-hand side of the equation, ground admittances Y_{30} and Y_{40}, as well as a ratio of the detector terminal potentials to V_1. If the ground admittances are zero or negligible, eq 5 reduces to

$$Y_{13}Y_{24}=Y_{23}Y_{14}, \quad (6)$$

involving only the admittances of the bridge proper. Relation 6 can also be made to apply by making $V_3=V_4=0$, which is the object sought in Wagner-grounded bridge technique. However, in high-precision work it may be difficult to balance the ground impedances to the same degree of precision as those in the bridge. This possibility can be seen in the equation

$$(Y_{10}+y_1)Y_{23}=(Y_{20}+y_2)Y_{13}, \quad (7)$$

which represents approximately the condition for $V_3=0$. The relation involves the admittances of the source, which admittances will, in general, be less stable than those of the bridge. When it is inconvenient to bring the detector to ground potential with the same precision as when the bridge proper is balanced, the equivalent effect can be obtained by making $(Y_{30}Y_{24}-Y_{40}Y_{23})$ so small that the right-hand side of eq 5 becomes negligible. The balance relation can then be represented by eq 6. In a bridge where stray admittances Y_{30} and Y_{40} are small compared with the admittances of the bridge, the balanced condition is much less dependent on the potential of the detector terminals with respect to ground than when these admittances are of the same order of magnitude. However, it is not generally realized that when the balance adjustments of the bridge

proper depend appreciably upon the values of Y_{10}, Y_{20}, y_1, and y_2 this dependence can be materially decreased by adjustment of either Y_{30} or Y_{40} to make

$$Y_{30}Y_{24} \cong Y_{40}Y_{23}. \tag{8}$$

This feature is especially useful in a bridge such as that shown in figure 1 arranged in the conjugate or low-voltage form where the dissimilarity of admittances Y_{23} and Y_{24} requires a corresponding dissimilarity in stray admittances Y_{30} and Y_{40} to reduce the dependence on the ground admittance values. Dye and Jones [7], using a conjugate-type Schering bridge, found that a resistance between ground and the junction of R_3 and R_4 considerably improved the performance of their bridge, but they did not point out the reason for it.

If an amplifier is used between the detector and bridge, the measurement of $(V_3 - V_4)$ directly requires either that the amplifier be ungrounded or that coupling between the bridge and amplifier be made through a shielded transformer of high impedance. The latter method is very unsatisfactory with a bridge where the high-impedance terminals are connected to the detector, primarily because of the influence of stray fields on the transformer. The use of an ungrounded, doubly shielded amplifier is preferable, and is the method described by Dye and Jones [7].

An alternate arrangement, permitting the use of a conventional grounded amplifier, involves adjusting the potentials of terminals 3 and 4 separately to ground potential. (This procedure will be referred to hereafter as separate balancing of the terminals to ground in contrast to a direct balance of the potentials of two terminals.) This procedure of course requires that the ground admittances be adjusted as carefully as those in the bridge proper, but frequently this will be more convenient than to use an ungrounded amplifier. Both methods have been used satisfactorily in the present work.

If the bridge is of the form shown in figure 1, specific admittance values may be substituted for the general terms of eq 6. The orientation of the bridge with respect to the source and detector is immaterial in this equation.

If the impurities in C_1 and C_2 are represented by equivalent parallel resistances R_1 and R_2, and if impurities in R_3 and R_4 are represented by equivalent parallel capacitances included in C_3 and C_4, eq 6 becomes, upon substituting proper values and separating the real and imaginary terms:

$$\frac{C_1}{R_4}+\frac{C_4}{R_1}=\frac{C_2}{R_3}+\frac{C_3}{R_2} \text{ and } \frac{1}{R_1R_4}-\omega^2C_1C_4=\frac{1}{R_2R_3}-\omega^2C_2C_3. \tag{6a}$$

The frequency of the alternating current is given by $\omega/2\pi$. If $C_1R_1 \gg C_4R_4$ and $C_2R_2 \gg C_3R_3$, eq 6a can be reduced and combined to give as the balance conditions

$$\frac{C_1}{C_2}=\frac{R_4}{R_3} \text{ and } \tan\phi_1-\tan\phi_2=\omega C_4R_4-\omega C_3R_3, \tag{6b}$$

where $\tan\phi_1$ and $\tan\phi_2$ are equal to $1/\omega C_1R_1$ and $1/\omega C_2R_2$, respectively, representing the tangents of phase-defect angles of C_1 and C_2. If these angles are small the tangents will be equal to the angles when

measured in radians, and they will also be equal to the power factors of the capacitors. An evaluation of the power-factor difference $(\phi_1-\phi_2)$ from the above equation requires an evaluation of the impurities or phase angles of R_3 and R_4, since these effects are included in C_3 and C_4. It is possible to determine $(\phi_1-\phi_2)$ independently of the phase angles of R_3 and R_4 by interchanging the connections to C_1 and C_2 with respect to R_3 and R_4. This interchange is also important in the elimination of the errors due to residual effects which result in an imperfect balance, and will be discussed in the next section.

(b) IMPERFECT BALANCE

The discussion so far has been based on the assumption that the bridge is balanced by either bringing both V_3 and V_4 to zero potential or by making V_3 exactly equal to V_4. In high-precision work these conditions are seldom, if ever, realized. Stray coupling to the detector or amplifier, or inductive coupling with the leads between the bridge and the detector or amplifier, may produce a deflection on the indicating instrument, even when no voltage is applied to the bridge. If such residual effects [3] are present a null indication by the detector when voltage is applied to the bridge will require an off-balance condition in the bridge to neutralize the deflections produced by the stray voltages. There is also a possibility that harmonics which may be present in the current from the source will combine in the amplifier to produce a fundamental which would in turn cause a deflection on a tuned indicator, even though the bridge were perfectly balanced for the fundamental frequency. This latter effect has been shown analytically by Goodhue [9] and experimentally by Ferguson and Bartlett [10] as well as during the course of this work. For this also a null indication would require an off-balance condition in the bridge for neutralization.

The error due to stray coupling may be eliminated by the well-known method [11] of reversing the connections between the bridge and the source. It will be shown that the same effect can be obtained by reversing the connections to C_1 and C_2 and that this reversal has the additional advantage of removing the necessity of evaluating the phase angles of R_3 and R_4. There is also some indication that the reversal of C_1 and C_2 eliminates any small harmonic-modulation error, although this latter effect is more surely removed by proper filtering both in the input to the bridge and in the various stages of a detector amplifier.

In order to determine the extent of the error produced by a residual deflection at balance, the bridge equations are written in a somewhat different form. An examination of the set of eq 4 shows that fourth-order determinants or their equivalents were encountered in obtaining relationships between the potentials of the bridge terminals and the bridge admittances. This was no great handicap in obtaining eq 5 from eq 4, because the equality $V_3=V_4$ was invoked. However, when neither the equality $V_3=V_4$, $V_3=0$, nor $V_4=0$ applies exactly, it is easier to handle two sets of three equations than one set of four. Two sets of three equations are obtained by setting up one set for the approximate balance of each of the detector terminals to ground. The results obtained apply equally to either of the previously men-

[3] These were referred to as parasitic voltages by Dye and Jones [7].

tioned methods of balancing the bridge; that is, when balancing each detector terminal separately to ground or the two terminals directly against each other. The set of equations from which the near-balance relationships for terminal 3 (fig. 2) can be derived are obtained by eliminating terminal 4 and all admittances terminating on it. The remaining admittances will all be modified by the elimination of terminal 4, and the amount of the modification can be determined by an equivalent circuit transformation. The new set of equations are taken directly from eq 4 by eliminating all terms containing V_4, Y_{14}, Y_{24}, Y_{34}, or Y_{40} and then modifying the remaining admittance terms. The result of these eliminations is as follows:

$$\left.\begin{aligned} &V_1(2Y_{123}+\overline{Y}_{13}+Y_{103})-V_2(2Y_{123}+\overline{Y}_{23}+Y_{203})+V_3(\overline{Y}_{23}-\overline{Y}_{13})=S_1\\ &V_1Y_{103}+V_2Y_{203}+V_3\overline{Y}_{30}=S_2\\ &V_1\overline{Y}_{13}+V_2\overline{Y}_{23}-V_3(\overline{Y}_{13}+\overline{Y}_{23}+\overline{Y}_{30})=0. \end{aligned}\right\} \quad (9)$$

The values of the modified admittance terms are defined as follows:

$$\left.\begin{aligned} Y_{123}&=Y_{12}+y_0+\frac{Y_{14}Y_{24}}{\Sigma_4} & \overline{Y}_{30}&=Y_{30}+\frac{Y_{34}Y_{40}}{\Sigma_4}\\ Y_{103}&=Y_{10}+y_1+\frac{Y_{14}Y_{40}}{\Sigma_4} & Y_{203}&=Y_{20}+y_2+\frac{Y_{24}Y_{40}}{\Sigma_4}\\ \overline{Y}_{13}&=Y_{13}+\frac{Y_{14}Y_{34}}{\Sigma_4} & \overline{Y}_{23}&=Y_{23}+\frac{Y_{24}Y_{34}}{\Sigma_4}\\ &\Sigma_4=Y_{14}+Y_{24}+Y_{34}+Y_{40} \end{aligned}\right\} \quad (10)$$

A similar set of equations may be obtained for the balance of terminal 4, by replacing the subscripts 3 by 4 and 4 by 3 in eq 9 and 10.

The relation between V_3 and the bridge admittances is obtained from eq 9 by the elimination of V_1 and V_2. The corresponding equation for V_4 may be obtained by the interchanging of subscripts. In writing these relationships it is convenient to define new admittance terms which are common to both equations. The equation involving V_3 is

$$Y_{103}\overline{Y}_{23}=Y_{203}\overline{Y}_{13}+\frac{S_2}{S_1}\left[2Y_x(\overline{Y}_{13}+\overline{Y}_{23})+Y_y\overline{Y}_{23}+Y_z\overline{Y}_{13}\right] \quad (11)$$

$$-\frac{2V_3}{S_1}Y_b(Y_x+Y_y)(\overline{Y}_{13}+\overline{Y}_{23}+\overline{Y}_{30}),$$

and for V_4 is

$$Y_{104}\overline{Y}_{24}=Y_{204}\overline{Y}_{14}+\frac{S_2}{S_1}\left[2Y_x(\overline{Y}_{14}+\overline{Y}_{24})+Y_y\overline{Y}_{24}+Y_z\overline{Y}_{14}\right]$$

$$-\frac{2V_4}{S_1}Y_b(Y_x+Y_y)(\overline{Y}_{14}+\overline{Y}_{24}+\overline{Y}_{40}), \quad (12)$$

where the new terms are defined as follows:

$$\left.\begin{aligned} Y_x &= Y_{123}+\frac{\overline{Y}_{13}\overline{Y}_{23}}{\overline{Y}_{13}+\overline{Y}_{23}+\overline{Y}_{30}} \equiv Y_{124}+\frac{\overline{Y}_{14}\overline{Y}_{24}}{\overline{Y}_{14}+\overline{Y}_{24}+\overline{Y}_{40}} \\ Y_y &= Y_{103}+\frac{\overline{Y}_{30}\overline{Y}_{13}}{\overline{Y}_{13}+\overline{Y}_{23}+\overline{Y}_{30}} \equiv Y_{104}+\frac{\overline{Y}_{40}\overline{Y}_{14}}{\overline{Y}_{14}+\overline{Y}_{24}+\overline{Y}_{40}} \\ Y_z &= Y_{203}+\frac{\overline{Y}_{30}\overline{Y}_{23}}{\overline{Y}_{13}+\overline{Y}_{23}+\overline{Y}_{30}} \equiv Y_{204}+\frac{\overline{Y}_{40}\overline{Y}_{24}}{\overline{Y}_{14}+\overline{Y}_{24}+\overline{Y}_{40}} \end{aligned}\right\} \quad (13)$$

and

$$Y_b = Y_x+\frac{Y_y Y_z}{Y_y+Y_z}. \quad (14)$$

Admittances Y_x, Y_y, and Y_z represent the effective values between the terminals 1 and 2, 1 and 0, and 2 and 0, respectively, upon elimination of junctions 3 and 4 by transformations of the star-delta type. The identities indicate that the same values are necessarily obtained regardless of the order in which terminals 3 and 4 are eliminated. Equation 14 gives the admittance of the entire bridge. Equations 11 and 12 can be combined to give

$$[\overline{Y}_{23}\overline{Y}_{14}-\overline{Y}_{24}\overline{Y}_{13}]\left[Y_y+Y_z+\frac{S_2}{S_1}(Y_z-Y_y)\right]=\frac{2Y_b(Y_y+Y_z)}{S_1}$$

$$\left[V_4(\overline{Y}_{13}+\overline{Y}_{23})(\overline{Y}_{14}+\overline{Y}_{24}+\overline{Y}_{40})-V_3(\overline{Y}_{14}+\overline{Y}_{24})(\overline{Y}_{13}+\overline{Y}_{23}+\overline{Y}_{30})\right], \quad (15)$$

which can be shown to be equivalent to

$$[\overline{Y}_{23}\overline{Y}_{14}-\overline{Y}_{24}\overline{Y}_{13}][V_1-V_2]=(V_4-V_3)(\overline{Y}_{13}+\overline{Y}_{23})(\overline{Y}_{14}+\overline{Y}_{24})$$
$$+V_4\overline{Y}_{40}(\overline{Y}_{13}+\overline{Y}_{23})-V_3\overline{Y}_{30}(\overline{Y}_{14}+\overline{Y}_{24}). \quad (15a)$$

In this form the equation may be readily reduced to eq 6 if V_3 and V_4 are zero or to a relation equivalent to eq 5 if $V_3=V_4$. If the equivalent admittance terms on the left-hand side of the equation are replaced by their actual admittance values, as defined by eq 10, then eq 15a may be written

$$(Y_{23}Y_{14}-Y_{24}Y_{13})=\frac{1}{(V_1-V_2)\left(1-\frac{Y_{34}{}^2}{\Sigma_3\Sigma_4}\right)}\Big[(V_4-V_3)(\overline{Y}_{13}+\overline{Y}_{23})(\overline{Y}_{14}+\overline{Y}_{24})$$
$$+V_4\overline{Y}_{40}(\overline{Y}_{13}+\overline{Y}_{23})-V_3\overline{Y}_{30}(\overline{Y}_{14}+\overline{Y}_{24})\Big]. \quad (16)$$

This equation now contains on the left-hand side only the admittances of the bridge proper, and on the right-hand side terms showing the effect of differences of V_3 and V_4 from each other and from ground potential. In a perfectly balanced Wagner-grounded bridge the right-hand side would of course be zero, but in the general case the equation serves to indicate the influence on the bridge proper of finite values for these potential differences. The right-hand side of eq 16 may then be considered as a correction term showing the error involved in assuming the left-hand side of the equation to be equal to zero. Approximations may now be made in this correction term and still allow an upper limit to be assigned to the effect of the residual

potential differences. One approximation is to neglect $Y_{34}^2/\Sigma_3\Sigma_4$ as compared to unity.

This is justified because Y_{34} represents the small admittance across the detector terminals composed mainly of the capacitance and leakage between the grid and cathode of a vacuum tube, whereas $\Sigma_3\Sigma_4$ contains such relatively large admittances as R_3 and R_4 (fig. 1). For the same reason, the barred terms representing the equivalent admittance values may be considered approximately equal to the unbarred terms representing the actual values (see eq 10). It should be pointed out that this approximation is required only in the right-hand side, or correction term, of eq 16. This equation can be arranged in a form more suitable for estimating the effect of residual potentials by transferring the $Y_{24}Y_{13}$ term from the left- to the right-hand side of the equation and then dividing both sides by $Y_{24}Y_{13}$. Doing this, and at the same time making the approximations outlined above, eq 16 becomes

$$\frac{Y_{23}Y_{14}}{Y_{24}Y_{13}}=1+\frac{1}{V_1-V_2}\left[(V_4-V_3)\left(1+\frac{Y_{23}}{Y_{13}}\right)\left(1+\frac{Y_{14}}{Y_{24}}\right)+\frac{V_4Y_{40}}{Y_{24}}\left(1+\frac{Y_{23}}{Y_{13}}\right)-V_3\frac{Y_{30}}{Y_{13}}\left(1+\frac{Y_{14}}{Y_{24}}\right)\right]. \quad (17)$$

In this form the correction term, when evaluated, gives directly the relative magnitude of the error produced by imperfect balance. Letting Y_{13} and Y_{23} represent the C_1 and C_2 branches of the bridge (fig. 1) and Y_{14} and Y_{24} the (R_3, C_3) and (R_4, C_4) branches, estimates of the error may be made. The correction due to a definite difference for (V_4-V_3) will be a minimum for a bridge symmetrical about the detector terminals ($C_1\cong C_2$). This correction is then four times the ratio of (V_4-V_3) to (V_1-V_2). The correction term due to the V_4 term alone will generally be much less than the V_4 to (V_1-V_2) ratio, because Y_{40}/Y_{24} will normally be appreciably less than unity. However, referring now to the V_3 correction term, the Y_{30}/Y_{13} ratio is apt to be near the order of unity, since both Y_{30} and Y_{13} are largely capacitance terms making this corrective term roughly of the same order as the $V_3/(V_1-V_2)$ ratio. The effect of individual values for V_3 and V_4 can, however, be neutralized by increasing Y_{40} in such a manner that

$$Y_{40}(Y_{13}+Y_{23})\cong Y_{30}(Y_{14}+Y_{24}). \quad (17a)$$

This requirement is equivalent to that expressed by eq 8, since $Y_{13}Y_{24}\cong Y_{14}Y_{23}$.

In order to reduce the effect of all residual potential differences, C_1 and C_2 or Y_{13} and Y_{23} are interchanged and the bridge readjusted to give the same values of V_3 and V_4. This simply means that the bridge is balanced as before and that the residual effects are not affected by the interchange. If rebalance is obtained by varying Y_{13}, Y_{14}, and Y_{10} by small amounts α, β, and γ so that

$$Y_{13}'=Y_{13}+\alpha;\ Y_{14}'=Y_{14}+\beta;\ \text{and}\ Y_{10}'=Y_{10}+\gamma,$$

the new equation for imperfect balance may be written

$$\frac{Y_{13}'Y_{14}'}{Y_{24}Y_{23}}=1+\frac{1}{(V_1-V_2)'}\left[(V_4-V_3)\left(1+\frac{Y_{13}'}{Y_{23}}\right)\left(1+\frac{Y_{14}'}{Y_{24}}\right)+\frac{V_4Y_{40}}{Y_{24}}\left(1+\frac{Y_{13}'}{Y_{23}}\right)-\frac{V_3Y_{30}}{Y_{23}}\left(1+\frac{Y_{14}'}{Y_{24}}\right)\right]. \quad (18)$$

The potential difference $(V_1-V_2)'$ will be related to the previous potential difference according to the ratio

$$(V_1-V_2)/(V_1-V_2)'=Y_b'/Y_b,$$

where the primed terms represent the values upon reversal. Since the correction terms are small, eq 17 and 18 may be combined to give

$$\frac{Y_{23}^2Y_{14}}{Y_{13}Y_{13}'Y_{14}'}=1+\left[\frac{V_4-V_3}{Y_b(V_1-V_2)}\right]\left[\left(1+\frac{Y_{23}}{Y_{13}}\right)\left(1+\frac{Y_{14}}{Y_{24}}\right)Y_b-\left(1+\frac{Y_{13}'}{Y_{23}}\right)\left(1+\frac{Y_{14}'}{Y_{24}}\right)Y_b'\right]+\frac{V_4Y_{40}}{Y_b(V_1-V_2)Y_{24}}\left(\frac{Y_{23}Y_b}{Y_{13}}-\frac{Y_{13}'Y_b'}{Y_{23}}+Y_b-Y_b'\right)-\frac{V_3Y_{30}}{Y_b(V_1-V_2)}\left[\left(1+\frac{Y_{14}}{Y_{24}}\right)\frac{Y_b}{Y_{13}}-\left(1+\frac{Y_{14}'}{Y_{24}}\right)\frac{Y_b'}{Y_{23}}\right]. \quad (19)$$

By substituting the above values for Y_{13}', Y_{14}', and Y_{10}', this may be reduced approximately to

$$\frac{Y_{23}^2Y_{14}}{Y_{13}Y_{13}'Y_{14}'}=1+\left(\frac{V_3-V_4}{V_1-V_2}\right)\left(\frac{\alpha+\beta+\gamma}{Y_b}\right)-\frac{V_4Y_{40}}{2(V_1-V_2)Y_bY_{24}}\left(\alpha-\frac{\beta Y_{13}}{Y_{14}}\right)-\frac{V_3Y_{30}}{2(V_1-V_2)Y_bY_{13}}\left(\frac{\alpha Y_{14}}{Y_{13}}+\frac{\alpha Y_{10}}{Y_{13}}-\beta-\gamma\right). \quad (20)$$

From this equation it may be seen that the effect of a (V_3-V_4) residual has been materially reduced, since the $(V_3-V_4)/(V_1-V_2)$ term is now multiplied by the small ratio of the sum of the admittance changes upon interchange to the total bridge admittance. The reversal or interchange procedure permits a high precision to be maintained with relatively large residual values for (V_3-V_4). For example, the (V_3-V_4) to (V_1-V_2) ratio may be as large as 1×10^{-3}, and if the admittance changes upon reversal are less than a thousandth of the total bridge admittance, the correction term will be less than 1 part in a million. The V_4 residual has also been reduced by approximately the same factor. The V_3 term, however, may still be important because the reduction effected by the α/Y_b multiplication has been offset by a further multiplication by Y_{14}/Y_{13}. Remembering that Y_{14} represents a resistance term and Y_{13} a capacitance term, it may be seen that this latter ratio might be quite large. The V_3 term then serves to define the upper limit of error which may be produced by the residual potential differences. If it can be shown that this term is negligible, the others quite certainly will be negligible also. The effect of this term can be controlled mainly by Y_{30}; hence it is good bridge technique to keep this admittance small. However, if an appreciable increase in Y_{30} fails to affect the value of the left-hand side of eq 20, one may be reasonably certain that residual effects are not influencing the bridge measurements. On the other hand, if this term is important it should be remembered that it can be neutralized by the V_4 term by the adjustment of Y_{40}, as previously pointed out. This would leave only the (V_3-V_4) term, which, it has been shown, is very small. It is now possible to write eq 20 in the form

$$\frac{Y^2{}_{23}Y_{14}}{Y_{13}Y'{}_{13}Y'{}_{14}}=1 \quad (20a)$$

and to determine the upper limit of any error involved in this simplification.

Returning now to fig. 1, and letting the losses in C_1 and C_2 be represented by equivalent parallel resistances R_1 and R_2, eq 20a becomes

$$\left(j\omega C_2+\frac{1}{R_2}\right)^2\left(j\omega C_3+\frac{1}{R_3}\right)=\left(j\omega C_1+\frac{1}{R_1}\right)\left(j\omega C_1'+\frac{1}{R_1}\right)\left(j\omega C_3'+\frac{1}{R_3}\right) \tag{21}$$

Equating the real and imaginary terms gives

$$\frac{2C_2R_2+C_3R_3-\omega^2C_2^2R_2^2C_3R_3}{R_2^2}=\frac{(C_1+C_1')R_1+C_3'R_3-\omega^2C_1C_1'R_1^2C_3'R_3}{R_1^2} \tag{22}$$

and

$$\frac{1-\omega^2C_2^2R_2^2-2\omega^2C_2C_3R_2R_3}{R_2^2}=\frac{1-\omega^2C_1C_1'R_1^2-\omega^2(C_1+C_1')C_3'R_1R_3}{R_1^2} \tag{23}$$

The phase-defect angles or power factors of C_1 and C_2 will again be represented by ϕ_1 and ϕ_2. If $\phi_1^2<1\times10^{-6}$, $\phi_2^2<1\times10^{-6}$, and $\phi_1-\phi_1'<1\times10^{-6}$, an error of less than 1 part in a million will be involved in simplifying eq 22 to

$$C_2^2(2\phi_2-\omega C_3R_3)=C_1C_1'(2\phi_1-\omega C_3'R_3). \tag{24}$$

If, in addition, $\phi_1\omega C_3R_3$ and $\phi_2\omega C_3R_3<1\times10^{-6}$, eq 23 may be written

$$C_2^2=C_1C_1', \tag{25}$$

which, when combined with eq 24, gives

$$2(\phi_2-\phi_1)=\omega R_3(C_3-C_3'). \tag{26}$$

The latter equation is the one used for determining power-factor differences, and it should be noted that it does not require evaluation of the phase angles of the ratio-arm resistors, but only the change in C_3 between the two balances.

The assumption in the preceding analysis that detector terminal potentials V_3 and V_4 are the same upon the reversal of C_1 and C_2 has not been established analytically for a residual effect due to harmonic modulation. Although, as will be explained later, precautions are taken to prevent the existence of such an effect, it has been found that when the harmonic content of the input voltage is increased sufficiently to alter the values of C_3 and C_3' for the two null indications, the difference (C_3-C_3') is unchanged.

2. HIGH-VOLTAGE, OR REGULAR SCHERING BRIDGE

When the power is applied to the bridge of figure 1 at the C_1, C_2, and R_3, R_4 junctions, it is not always possible to bring the detector terminals to ground potential by use of a Wagner-grounding arm containing only resistance and capacitance. This may be seen from eq 7, which may be written in the form

$$Y_{23}/Y_{13}=(Y_{20}+y_2)/(Y_{10}+y_1),$$

and which represents the approximate condition for bringing a detector terminal (terminal 3, fig. 2) to ground potential. Admittances Y_{13} and Y_{23} represent, in the high-voltage form of the bridge, primarily a resistance term and a capacitance term, respectively, and

hence are considerably different in magnitude. The left-hand side of the above equation will then consist mainly of a term of the form $j\omega CR$. On the other hand, when y_1 and y_2 are not negligible the right side of the above relation may have an appreciable real component in addition to the imaginary component. Under such circumstances the relation can be satisfied only by reduction of the real component within the right-hand side of the equation. It can be shown that this will generally require an inductance in the ground arm which, as previously mentioned, is not desirable. In order to avoid using inductances in the bridge, Ogawa has suggested the insertion of an impedance in the power line lead between the C_1, C_2 junction in the bridge proper and the grounding arm. By making this addition to the bridge we will have a general network, as shown in figure 3 (a).

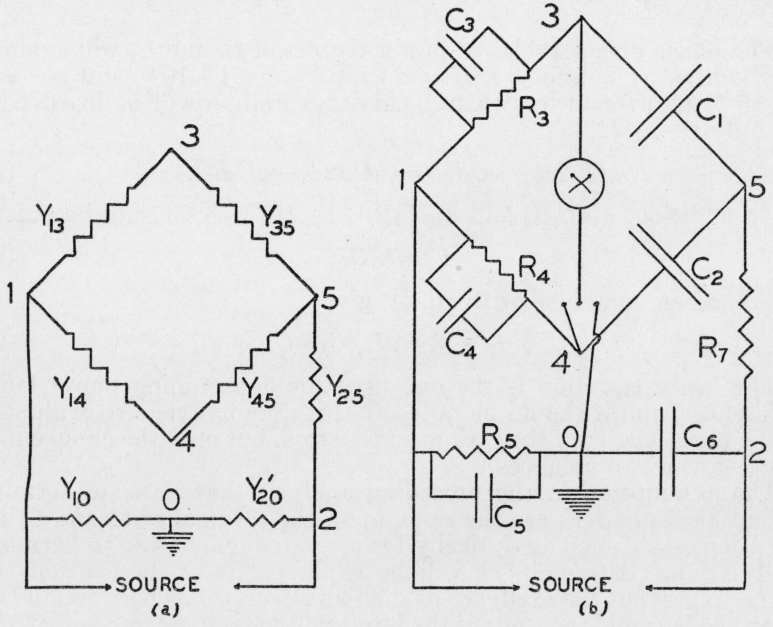

FIGURE 3.—*High-voltage type Schering bridge with Wagner ground.*

General admittances shown in (*a*), specific admittances in (*b*).

(The stray admittances are not indicated.) If terminal 5 is eliminated by an equivalent circuit transformation we will have a circuit of the same form as shown in figure 2 but in which the impedances have the following values

$$\left.\begin{aligned} Y_{23} &= \frac{Y_{35}Y_{25}}{\Sigma_5} \\ Y_{24} &= \frac{Y_{45}Y_{25}}{\Sigma_5} \\ Y_{20} &= Y_{20}' + \frac{Y_{50}Y_{25}}{\Sigma_5}, \end{aligned}\right\} \tag{27}$$

where $\Sigma_5 = Y_{25} + Y_{35} + Y_{45} + Y_{15} + Y_{50}$. Stray admittances Y_{30}, Y_{40}, and Y_{12} will also be slightly modified by the transformation, but we can

disregard these changes for the following discussion. All the equations previously developed will now apply if we substitute the above equivalent values in the equations. The balance relation, eq. 5, becomes

$$(Y_{13}Y_{45}-Y_{14}Y_{35})=\frac{V_3+V_4}{V_3+V_4-2V_1}(Y_{40}Y_{35}-Y_{30}Y_{45}), \tag{28}$$

and the approximate condition for $V_3=0$, previously represented by eq 7, is

$$(Y_{10}+y_1)Y_{35}Y_{25}=[(Y_{20}'+y_2)\Sigma_5+Y_{50}Y_{25}]Y_{13}. \tag{29}$$

If the actual admittances are as shown in figure 3 (b), the approximate conditions for bringing terminal 3 to ground potential are

$$\frac{\omega^2C_5'C_1}{R_7}+\frac{1}{R_6'R_3R_7}=\frac{\omega^2C_6'(C_1+C_2)}{R_3} \tag{30}$$

and

$$\frac{C_1}{R_7R_5'}=\frac{C_6'}{R_3R_7}+\frac{C_1+C_2}{R_3R_6'}. \tag{31}$$

In obtaining the above equations, the effects of stray admittances were neglected and the source admittances were included in C_5, C_6, R_5, and R_6, which was indicated by the priming of the terms. These equations serve to indicate the values of ground impedances required to obtain this balance. If the insulation resistance of the source is very high, and if $C_1\cong C_2$, the equations may be further simplified to

$$\frac{C_5'}{R_7}=\frac{2C_6'}{R_3} \text{ and } \frac{C_1}{R_5'}=\frac{C_6'}{R_3} \tag{32}$$

With this type of bridge, which offers a low impedance to the detector, connection is best made to the detector or amplifier through a shielded transformer. Consequently the most desirable procedure in balancing is to compare terminals 3 and 4 directly and balance only one of them against the ground terminal. Furthermore, it is not necessary to make the ground balance with high precision because, referring to eq 28, the admittance products on the right-hand side of the equation will be much smaller than those on the left-hand side; also the difference of the products may be small because of the symmetry of the terms. If, for example, admittances Y_{13} and Y_{14} are a thousand times larger than admittances Y_{30} and Y_{40}, the potential of the detector terminals can be as much as a thousandth part of the potential drop across Y_{13} or Y_{14}, and still the simple balance relation $Y_{13}Y_{45}=Y_{14}Y_{35}$ will apply with an error of less than 1 part in a million.

The equations for imperfect balance developed for the low-voltage bridge can be made applicable to the high-voltage form by substituting the values of eq 27 in eq 17. Reversal is then obtained by interchanging Y_{35} and Y_{45} and readjusting Y_{45}, Y_{14}, and Y_{10} by amounts δ, ϵ, and ζ. The final equation is

$$\frac{Y_{35}^2Y_{14}}{Y_{45}Y_{45}'Y_{14}'}=1+\frac{(V_3-V_4)}{(V_1-V_2)Y_b}\left(\frac{\delta Y_{25}}{\Sigma_5}+\epsilon+\zeta\right)$$
$$+\frac{V_4Y_{40}}{(V_1-V_2)Y_bY_{14}}\left(\frac{\epsilon Y_{10}}{Y_{14}}+\frac{\epsilon Y_{13}}{Y_{14}}-\zeta\right)+\frac{V_3Y_{30}}{(V_1-V_2)Y_bY_{13}}(\epsilon+\zeta) \tag{33}$$

It can be seen from this equation that the effect of small values for V_3 and V_4 will be less for this form of bridge than the other. Upon substituting specific values in the left-hand side of the equation it becomes identical to the relation obtained for the conjugate form of the bridge, so the same balance equations will apply when residual effects are negligible.

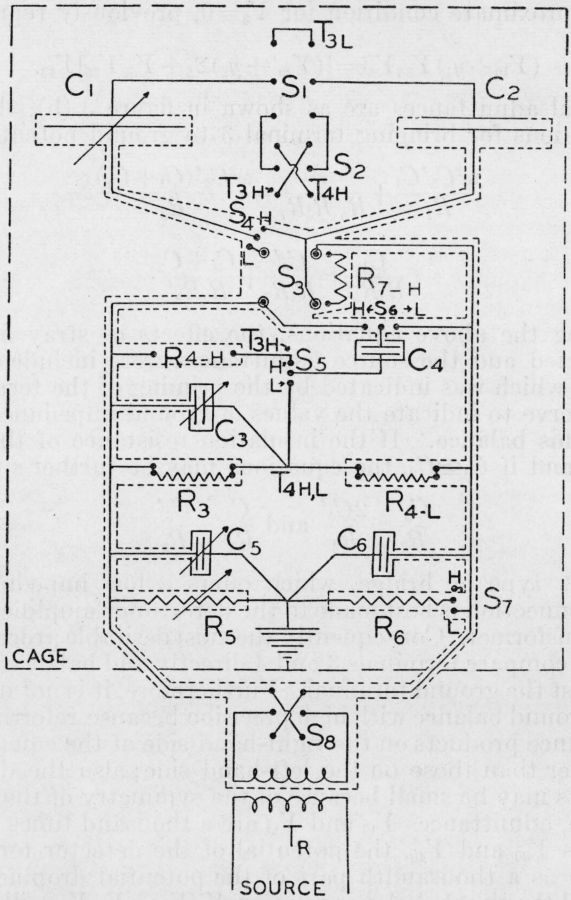

Figure 4.—*Circuit diagram of the bridge, showing switches for changing from a high-voltage to a low-voltage bridge.*

The detector terminals for the low-voltage bridges are labeled T_{3L} and T_{4HL} and for the high-voltage bridge T_{3H}, T_{3H} and T_{4H}, T_{4HL}. Commutator S_3 interchanges C_1 and C_2 in the low-voltage bridge and in the high-voltage bridge the interchange is accomplished by switch S_2.

III. DESCRIPTION OF THE BRIDGE

The general arrangement of the component parts of the bridge is shown in figure 4. Also shown are the switches for obtaining the low-voltage or high-voltage form of the bridge as well as the reversing switches for the elimination of residual effects. Shielding requirements necessitate a fixed orientation of the bridge impedances with respect to the source and detector, so that the change from one bridge

form to another cannot be obtained by a simple 90° rotation of the bridge assembly, as one might suppose from the discussion of figure 1. Capacitors C_1 and C_2 are of the three-electrode type with all the insulation at the grounded electrode, so that the leakage resistance is in parallel with R_5 and R_6 and does not influence the bridge proper. These capacitors will be described in detail later. Not shown is a small vernier guard-ring capacitor in parallel with C_1, which permits adjustment of the total capacitance to a few parts in 10 million.

Resistors with a Curtis-type winding [12] to give a small phase angle are used for R_3 and R_4. They are arranged to plug into jacks to facilitate their replacement. For observations at 60 c/s, 10,000-ohm resistors are used, but at 200 and 1,000 c/s these were replaced by 1,000-ohm coils. R_4 is shown in its position in the low-voltage bridge. Its position in the high-voltage bridge is indicated by R_{4H}. Capacitors C_3 and C_4 are two-electrode air capacitors with Isolantite insulation. Capacitor C_4 is variable between 50 and 1,500 $\mu\mu$f. Capacitor C_3, on which the power-factor differences are measured (eq 26), has two ranges, one from 25 to 100 $\mu\mu$f and one from 50 to 1,100 $\mu\mu$f. The smaller range scale is so graduated that changes of a hundredth of a micromicrofarad are readable. Thus, at a frequency of 60 c/s and with resistors of 10^4 ohms in the bridge, power factors of less than 10^{-7} could be observed if the stability and sensitivity of the rest of the bridge warranted. It is essential that the capacitances of C_3 and C_4 as well as the phase angles of R_3 and R_4 be as small as possible, consistent with the magnitude of the power factors under observation in order to justify the approximation made in the section on bridge theory that

$$\phi_1 \omega C_3 R_3 < 1 \times 10^{-6}.$$

In the ground arm, R_6 is a fixed resistor of 10,000 ohms, and R_5 is a variable six-dial 10,000-ohm shielded resistance box. In series with it for small adjustments of hundredths of an ohm or less is a mercury slide-wire resistor [13]. Capacitors C_5 and C_6 are similar to C_4. For the high-voltage form of the bridge a variable decade mica capacitor with a total capacitance of 1μf is required in addition to the air capacitor in C_5.

The input transformer, T_r has a 1:1 ratio with a shield between the windings. A variable-ratio transformer is used between the input transformer and the source for adjustment of the input voltage. When using high voltage on the bridge a step-up transformer is inserted between the shielded transformer and the bridge.

The detector terminals for the low-voltage bridge are labeled T_{3L} and $T_{4H,L}$. For the high-voltage bridge the two T_{3H} points are connected together for one detector terminal and the T_{4H} and $T_{4H,L}$ terminals form the other detector connection. The last two pairs of terminals are permanently connected together, but the joining lines are omitted from the figure to avoid the confusion due to extra lines.

In the low-voltage form of the bridge, switch S_1 is in the upward position joining C_1 and C_2 to the detector terminal T_{3L}. Commutator S_3 is for interchanging C_1 and C_2; the connecting bars are vertical for the direct connection and horizontal for reversal. Switches S_4, S_5, S_6, and S_7 are on the L terminals.

In the high-voltage bridge, S_1 is in the down position and S_2 reverses the capacitor connections. In S_3, a resistor, R_7, of about 1 megohm

is inserted as indicated and the other switches are put on the H terminals. Both S_3 and R_7 are enclosed in a grounded shield.

The switch, S_8, may be used for reversing the input connections, but since this procedure accomplishes nothing that is not gained in the reversal of the capacitor connections, it is not essential.

In addition to the shielding shown on the various bridge admittances, the entire bridge beyond switch S_8 is enclosed in a bronze-wire cage large enough to include an operator. The cage eliminates the necessity of ground shields around C_3 and C_4 as well as around the detector terminals and switches, thus keeping the Y_{30} term (eq 20) from becoming too large. It is, however, essential that the detector terminals be placed on grounded plates to eliminate any possible leakage paths between them and the power lines. For example, before this was done a leakage path existed (in the low-voltage form of the bridge) across the insulation of the R_{4H} gap to T_{3H} and across the insulation (a table top) between T_{3H} and T_{3L}. This increased the apparent power factor of C_1 or C_2, depending on the connection in S_3. This error would normally be eliminated by the reversal procedure, but the nature of the leakage was so erratic that a precise power-factor balance was not always possible. Placing the switches on a grounded guard plate eliminated the difficulty. It is also essential that no part of the power leads be exposed to the C_1 or C_2 detector terminals, especially if there is insulation in the exposed field. The effect of such an exposure is to add a small capacitance having a very large power factor in parallel with either C_1 or C_2. This of course means that such switches as S_4, S_6, and S_7 as well as S_3 should be completely shielded.

A photograph of the complete bridge and detector layout is shown in figure 5. The arrangement was not intended to be compact but rather to provide space for flexibility in the choice of bridge parts, especially in permitting capacitors of various sizes and shapes to be connected in parallel with C_1 and C_2.

IV. THE DETECTOR CIRCUITS

Vibration galvanometers were used as the ultimate detectors at the frequencies at which the bridge was most frequently used, namely, 60, 200, and 1,000 cycles. For different frequencies in the same range a cathode-ray oscillograph was used. For much higher frequencies the heterodyne method of detection used by Dye and Jones [7] is recommended. In all cases amplification of the signal from the bridge is essential. The amplifier which was used for the frequencies in the commercial- and audio-frequency range is shown in figure 6, and the various modes of connecting the amplifier to the bridge are indicated in figure 7.

The amplifier was a conventional three-stage resistance-capacitance coupled type with two filter units, F_1 and F_2, which are adjusted for the frequency applied to the bridge. The filter, F_1, includes the coupling capacitor between the second and third stages. It was found neither necessary nor advisable to place the tuning units in the earlier stages of the amplifier. The harmonic modulation error, which the tuning units help to reduce, increases as a power greater than one of the signal strength and would therefore be produced largely in the last stage. The filter unit, F_1, tends to allow only the fundamental

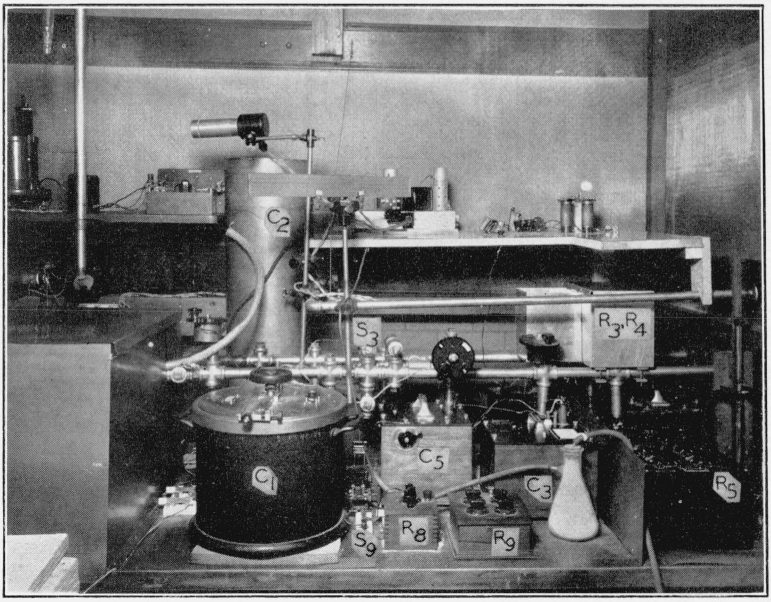

FIGURE 5.—*View of the bridge from the door of the enclosing, shielding cage.*

Designations correspond to objects shown diagrammatically in figures 4, 6, and 7.

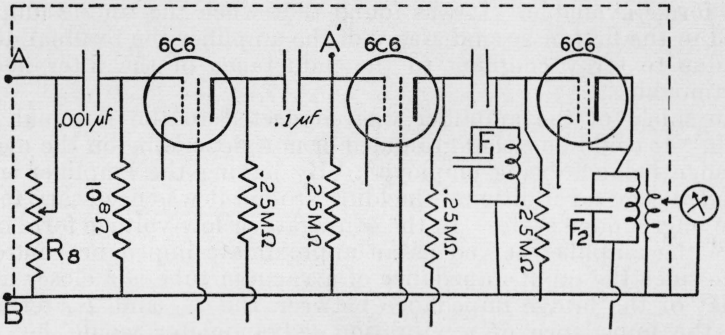

FIGURE 6.—*Circuit diagram of the amplifier and vibration galvanometer which comprise the bridge detector.*

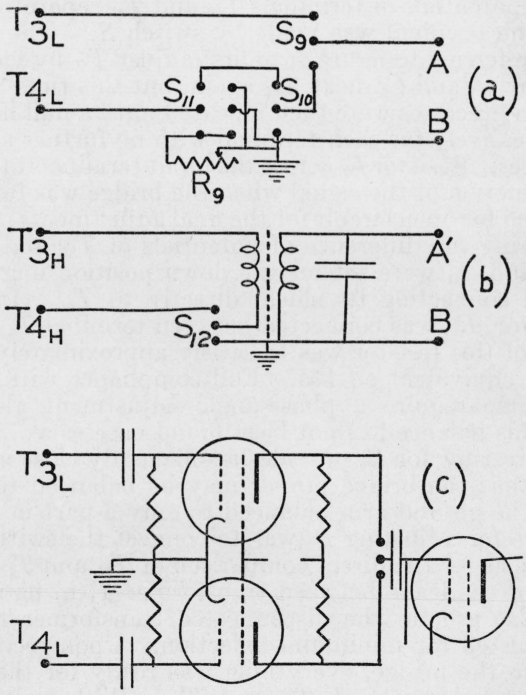

FIGURE 7.—*Methods of connecting the bridge to the detector.*

Terminal designations correspond to figures 4 and 6. The low-voltage bridge connections are shown in (*a*), where S_9 permits selection of the terminal to be balanced and S_{10} and S_{11} permit selection of the balance procedure. With S_{10} and S_{11} upward the amplifier is grounded and the bridge terminals are balanced separately to ground. In their downward positions the amplifier is ungrounded and the bridge terminals are compared directly. Stray admittance effects are neutralized by R_9. The high-voltage bridge connections are shown in (*b*). The switch, S_{12}, permits balance of the bridge proper or of the ground admittances. An alternate method for the low-voltage bridge of balancing the terminals separately against ground is indicated in (*c*).

to enter the last stage of amplification, and with the filter at this point no trouble was experienced from modulation error with the voltage wave forms available. It was found that when the tuning unit was placed in the first or second stages of the amplifier the residual deflection due to stray coupling to the inductance of the filter became objectionable.

The shield of the amplifier was connected to the terminal B as shown. It could be either grounded or not, depending on the method of bridge balance being employed. By having the amplifier in the grounded cage no additional shielding around it was necessary for use in the ungrounded state. In the conjugate or low-voltage form of the bridge the amplifier served as an approximate impedance matching device since the input impedance of a vacuum tube is a closer match to that of the bridge impedance between the T_{3L} and T_{4L} terminals than the impedance of a vibration galvanometer would be. The methods of connecting the amplifier to the low-voltage bridge are shown in figure 7 (a). With switches S_{10} and S_{11} in the upward position the amplifier was grounded and the bridge was balanced by adjusting the potentials of terminals T_{3L} and T_{4L} separately to ground. Selection of the terminal was made by switch S_9. The procedure of balance was, referring to figure 4, to first adjust T_{4L} by varying R_5 and C_5, then T_{3L} by C_1 and C_5, next T_{4L} again, but this time by C_3 and R_5. The latter two processes were then repeated until a null indication was obtained successively for each terminal with no further adjustment of the admittances. Resistor R_8 across the input terminals of the amplifier permitted reduction of the signal when the bridge was far off balance. It was arranged for open circuit for the final adjustments.

For comparing the difference of potentials of T_{3L} and T_{4L} directly, switches S_{10} and S_{11} were set for the down position ungrounding the amplifier and connecting its shield directly to T_{4L}. In addition, a variable resistor, R_9, was connected between terminal T_{4L} and ground. The purpose of this resistor was to satisfy approximately the relation of eq 8 or its equivalent eq 17a. Full compliance with this relation would of course require a phase-angle adjustment also, but such precision in this balance has not been found necessary. In general, a three-decade resistor for R_9 provides a sufficiently close adjustment of relation 17a that the bridge proper may be balanced to a part in a million with the ground arm balanced to only a part in 10 thousand. The procedure for adjusting R_9 was to connect the switches in figure 7 (a) the same as for the direct comparison of T_{3L} and T_{4L}, then to disconnect one of the leads between transformer T_r in figure 4 and the bridge and also ground the disconnected transformer terminal. R_9 was then adjusted for minimum deflection. Upon reconnecting the transformer to the bridge, everything was ready for the direct comparison of the potentials of T_{3L} and T_{4L}. With switch S_9 in the upward position the bridge proper was balanced, and in the lower position the ground arm was balanced. An alternate procedure was to put S_9 in the upward position, S_{10} in the downward position, and balance the bridge proper with S_{11} down and the ground arm with S_{11} up.

The question arose during the course of this work as to the possible effect of the input amplifier impedance upon the balance when the balance was not perfect and when terminals T_{3L} and T_{4L} were balanced individually to ground. The transferring of the amplifier connection

from one terminal to the other for each balance adjustment added and subtracted the input admittance of the amplifier successively to Y_{30} and Y_{40} and prevented a true simultaneity of the values in the equations for the two balances. Of course, if the amplifier admittance was sufficiently small the effect would be negligible. In order to check this point the input stage of the amplifier was arranged as shown in figure 7 (c). Here admittances Y_{30} and Y_{40} were the same for each balance and the selection of the terminal to be balanced was made by the switch as shown between the first and second stages of the amplifier. Identical results were obtained by each method so the single-tube procedure was considered sufficiently accurate.

In the high-voltage form of the bridge a low impedance is presented to the amplifier, so that an efficient transfer of signal strength requires a step-up transformer preferably with a shield between the primary and secondary windings. The method of connection and balance procedure is indicated in figure 7 (b). Bridge terminals T_{3H} and T_{4H} are balanced directly, and the switch S_{12} permits connecting one of the terminals for the ground balance. The use of the transformer permits grounding the amplifier. Here it is not necessary to adjust Y_{30} or Y_{40}, because these admittances will normally be much smaller than Y_{13} and Y_{14}, making this form of the bridge automatically much more independent of the ground balance. If a further increase of the independence of ground balance is desired, a variable capacitance between either terminal T_{3H} or T_{4H} and ground is indicated. The amount of amplification required with the high-voltage bridge will generally be less than for the low-voltage form, so that one stage of amplification may be dropped. This, in turn, will permit the use of a tuned unit in the input stage as shown. This is in general desirable because the wave form of the high voltage supplied to the bridge is apt to contain more harmonics than a low voltage.

V. THE LOW-LOSS CAPACITORS

As pointed out previously, it is highly desirable to make all balance adjustments in the bridge proper by varying capacitors only. The conventional variable capacitors were all of the two-electrode type and the use of such capacitors for C_1 and C_2 would mean the introduction of solid insulation in the low-loss measuring circuit of the bridge. Tests soon showed that such capacitors were unsatisfactory for power-factor measurements to 1×10^{-6}. In figure 8 is shown the variation, with scale setting and time, of the power-factor *difference* of two conventional two-electrode capacitors. The points indicate a series of observations covering about 2 hours' time, for decreasing and then increasing capacitance. The discrepancy between the two curves is due to the variation of the effective difference in leakage resistance of the two capacitors during the time interval between the two sets of measurements. The vertical line at the 1,350 $\mu\mu$f setting indicates the range of values observed for this setting of the capacitors during a 2-day period. The dashed line indicates a computed power-factor difference due to fixed parallel resistances.

In view of such unsatisfactory power-factor stability with conventional variable capacitors, it was considered essential to build a variable capacitor with no solid insulation between the measuring

electrodes. Such a condenser is illustrated in figure 9. It is of the common rotating-electrode type but with a third electrode, 10, introduced, which prevents a leakage path through solid insulation between the rotor system, 4, and the stator system, 12. This third electrode is grounded together with the outer case, 1. The capacitor was built with due consideration for mechanical stability in order that it might serve also as a reasonably precise variable standard of capacitance. The minimum and maximum capacitances are 86 and 1,946 $\mu\mu$f, respectively, and the range over which the capacitance variation with scale setting is linear is about 1,500 $\mu\mu$f. Scale 8 is a theodolite circle and is read on a vernier, 9. Angular changes of 10 seconds

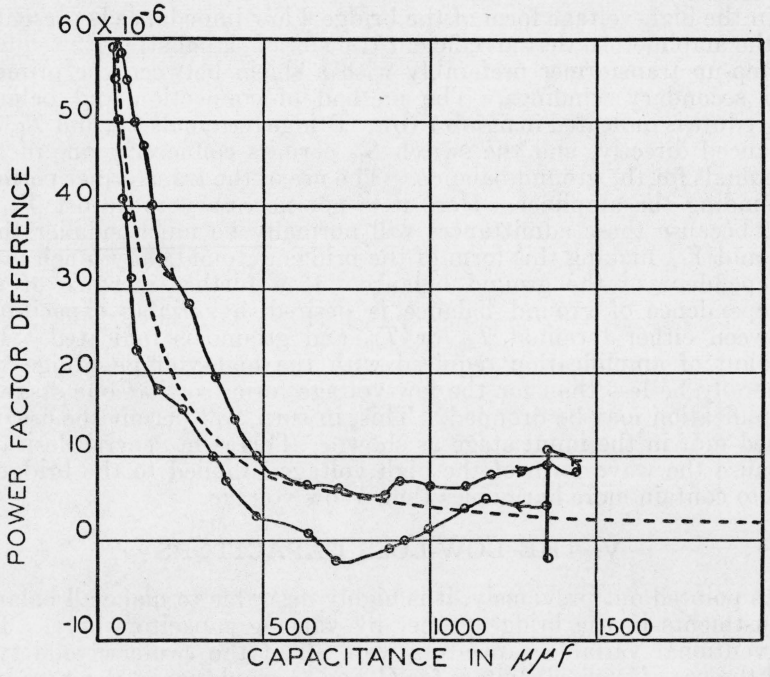

FIGURE 8.—*Power-factor differences of two air capacitors with Isolantite insulation.*

The dashed line indicates computed power factors due to assumed parallel resistances. The differences between the two solid-line curves show variations with time. The solid vertical line at 1,350 $\mu\mu$f shows the range of power-factor values observed during a 2-day period.

corresponding to capacitance changes of about 0.03 $\mu\mu$f may be read. The electrodes are of 1-mm brass, nickel-plated. They are so spaced that when the rotor and stator are interleaved there is an electrode separation of about 3 mm. This spacing is about three times that found in most commercial two-electrode rotating-plate capacitors. The electrode spacing was increased to reduce the effect of dust accumulation and electrode surface films upon the phase defect angle of the capacitor and incidentally to permit its use at higher voltages.

When placed in the bridge, the rotor was connected to the detector terminal, thus bringing it approximately to the potential of the grounded case at balance and the stator was connected to the power-line terminal. A better design might have been to decrease the

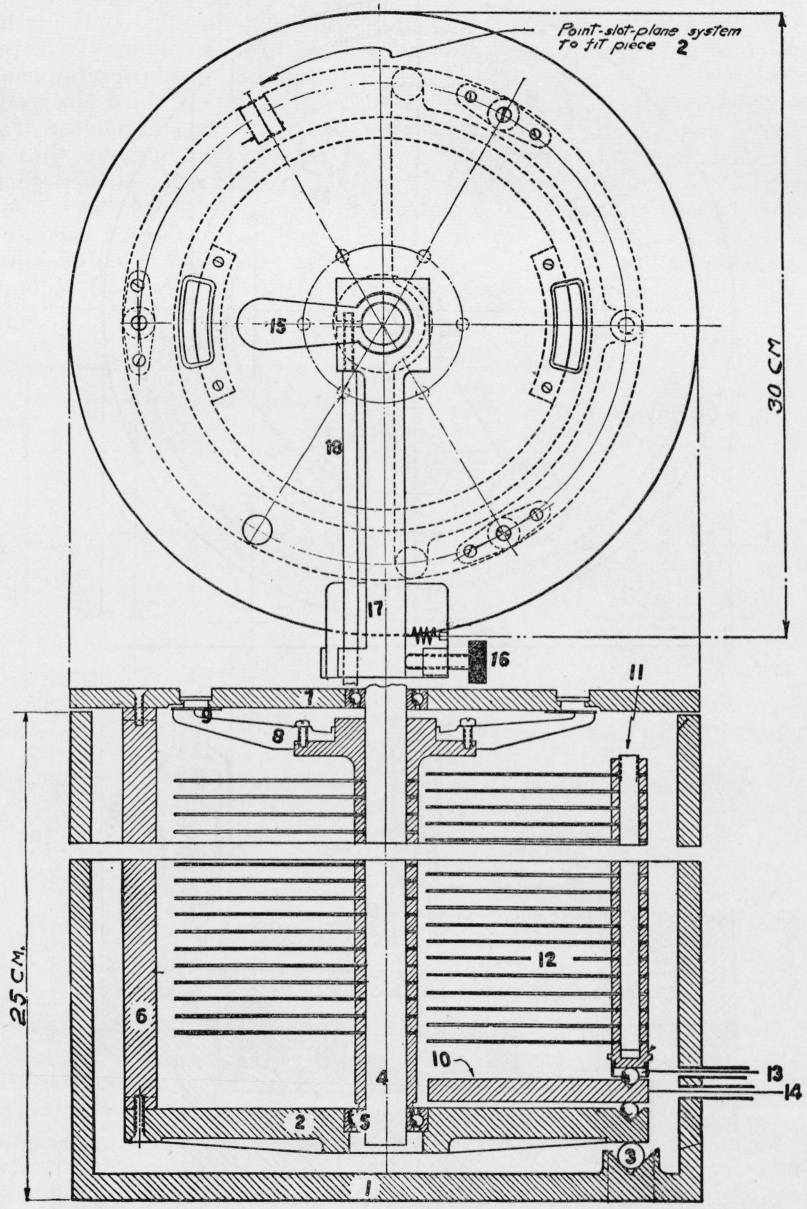

FIGURE 9.—*Plan and section of the three-terminal variable capacitor.*

The case, 1, serves as a grounded shield for the capacitor and supports the ribbed plate, 2, by three small quartz balls, 3, arranged in a hole-slot-plane system. The plate, 2, supports the rotor shaft, 4, by means of the steel ball bearing, 5. Three uprights, 6, support a top plate, 7, which carries a steel ball bearing providing an upper support for the rotor shaft. The top plate also carries the vernier index, 9, used in conjunction with the theodolite circle, 8, attached to the rotor shaft. A grounded-guard electrode, 10, rests on three quartz balls supported by plate, 2, and arranged in a hole-slot system. This guard electrode supports the three uprights, 11, of the stator system, 12, by quartz balls in a hole-slot-plane system. The lead wire, 13, permits connection to the stator system, and 14 is the grounding lead to the guard electrode. The connection to the rotor system is made through a binding post (not shown) on the top plate, 7. Coarse adjustments of the rotor are made by the handle, 15, and fine adjustments by the action of a screw, 16, on a lever arm, 17, which is held against the screw by a spring. Another screw, 18, permits clamping or unclamping the lever arm to or from the rotor shaft.

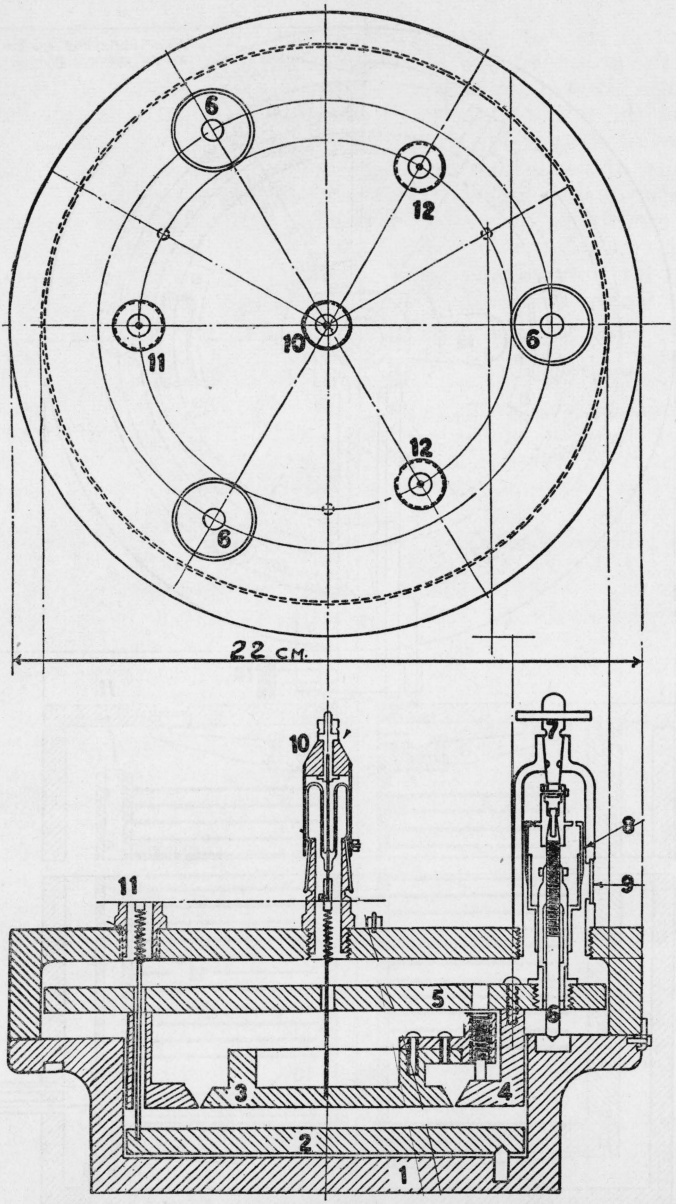

FIGURE 10.—*Plan and section of Gardiner's guard-ring, vacuum capacitor.*

The measuring electrodes are completely enclosed by the air-tight grounded case 1. The high-voltage electrode, 2, rests in the bottom of the case on three quartz balls (although pins are indicated in figure) arranged in a hole-slot-plane system. The low-voltage electrode, 3, is supported by quartz balls on the guard electrode, 4, which in turn is carried by the plate, 5. The vertical position of the 3, 4, and 5 assembly relative to the outer case and lower electrode is controlled by three micrometer screws, 6. A metal cone, 7, makes a vacuum fit in a cylindrical projection, 8, of the grounded outer case and permits turning of the micrometer screw without the breaking of the vacuum seal. The position of the micrometer may be read through the glass window, 9. A glass tube carrying a tungsten-glass seal, 10, permits electrical connection to be made to the low-voltage measuring electrode. The inner surface of the glass tube is ground to fit tightly on a metallic projection in the top of the case. A metal tube surrounds the glass tube to provide proper shielding for the electrode lead. Connection to the high-potential electrode is made at 11 in the same manner. Similar ground-glass inlet tubes, 12, provide means for filling or emptying the interior of the capacitor. The case and electrodes of the capacitor are made of Tobin bronze.

diameter of the top plate, which is part of the rotor system and to extend the grounded case above and over it to provide more thorough shielding. However, with the top plate connected to the detector terminal the major objection to its present form is the capacitative influence of stray fields on the residual deflection. Since it has been used only in the bridge in the grounded cage previously mentioned, this feature has not proved to be a handicap.

The guard-ring capacitor shown in figure 10 [4] has been used as another type of low-loss capacitor. This capacitor is suitable as a test cell for liquid dielectrics and also for gases since it was built for vacuum work. Because of a continuously variable electrode separation, capacitance values from 10 to several thousand microfarads are obtainable.

Also available as an auxiliary low-loss capacitor of fixed value was the cylindrical guard-ring capacitor used by Rosa and Dorsey in their work on the ratio of the electrical units [14]. This capacitor has a capacitance of about 150 $\mu\mu$f and an electrode separation of about 1 cm. The electrodes surfaces are silver-plated.

VI. DETERMINATION OF TRUE POWER-FACTOR VALUES

When any two of the three capacitors just described were placed in the bridge in the C_1 and C_2 positions it was found that their power-factor difference was not zero. It was furthermore found that the power-factor difference of the two variable capacitors changed with scale setting. The nature of the variation was such as to indicate either that the power factor of the rotating-electrode capacitor decreased with increasing capacitance or that the power factor of the guard-ring capacitor of variable electrode separation increased with increasing capacitance. It thus became apparent that in order to secure a satisfactory standard for power factor it was necessary to first determine the rate of variation of power factor with capacitance for a single capacitor. Then, if a sufficiently simple law of variation be observed it may become possible to extrapolate for the true values.

The variation of power factor with capacitance may be determined as follows: Let ϕ_{S1} be the phase-defect angle or power factor of the capacitor under investigation at a particular scale setting. Let ϕ_{A1} and ϕ_{B1} be the power factors of two other capacitors having the same capacitance as the first at the setting corresponding to ϕ_{S1}. Then the power factor differences $\phi_{S1}-\phi_{A1}=M_1$ and $\phi_{S1}-\phi_{B1}=M_2$ may be measured in the bridge. The two auxiliary capacitors are then connected in parallel, and it is a simple matter to show that the power factor of the combination will be the arithmetical mean of their individual values. The test capacitor is then varied to match the capacitance of the auxiliaries and the power factor difference $\phi_{S2}-(\phi_{A1}+\phi_{B1})/2=M_3$, measured. Here ϕ_{S2} is the power factor of the test capacitor at its new setting. This equation can be combined with the two previous ones to give

$$\phi_{S1}-\phi_{S2}=\frac{M_1+M_2}{2}-M_3, \tag{34}$$

[4] This capacitor was designed by and built under the direction of G. W. Gardiner, Jr. while he was at the National Bureau of Standards as a research associate representing the Utilities Research Commission of Illinois. It was intended primarily for studying ionic mobilities in very highly insulating liquid hydrocarbons from direct-current conduction measurements.

which represents the change in power factor of the test capacitor between the two scale settings. If the auxiliary capacitors are adjustable over a wide enough capacitance range the variations in the test capacitor can be determined over its entire scale. Such a calibration for the rotating-plate capacitor of figure 9 is shown in figure 11 for two frequencies of measurement, namely, 60 and 1,000 c/s. The zero point for the power-factor scale is of course entirely arbitrary, changes only being significant. It will be noted that the decrease of power factor with capacitance and frequency as well as the decrease of the rate of power factor change with capacitance are somewhat similar to the effect of a resistor in parallel with the capacitor. Used as auxiliary capacitors in this calibration were the guard-ring capacitor shown in figure 10 and a commercial two-

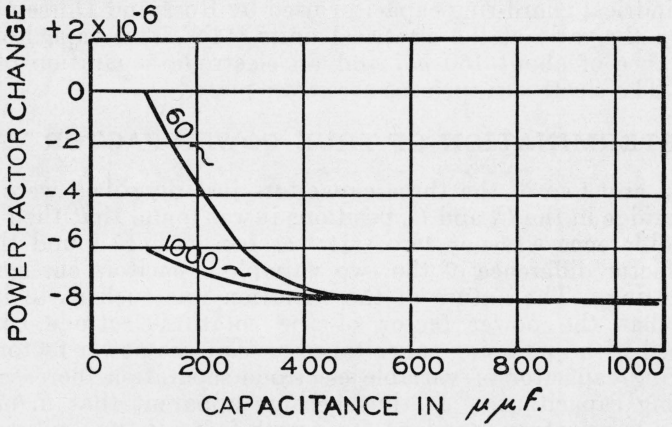

FIGURE 11.—*Change in power factor with scale setting of the three-terminal variable capacitor of figure 9.*

electrode capacitor with quartz insulation. When used in a reasonably dry atmosphere this latter capacitor had appreciably greater stability than those whose stability is illustrated in figure 8.

A similar power-factor calibration of the variable guard-ring capacitor could be made, but it was found more convenient to compare it directly with the rotating-plate capacitor, using its calibration curve shown in figure 11. This procedure requires (a) the selection of some point on the curve of figure 11 as a reference position and (b) the determination of differences of the power factors of the guard-ring capacitor at various scale settings with respect to this point. A plot of the power-factor variations of this instrument at frequencies of 60, 200, and 1,000 c/s is shown in figure 12. The zero point for the ordinate scale is taken as the power factor of the rotating-electrode capacitor at 150 $\mu\mu f$. The observed points lie very closely on a straight line, indicating a linear variation of power factor with capacitance, such as one might obtain with a fixed series resistor.

In order to establish definitely the linear variation of the power factor of a guard-ring capacitor with capacitance or inverse electrode separation, it is essential to show that the effect is independent of the gradient. This is especially important inasmuch as Balsbaugh [3] has also observed the power-factor increase of a guard-ring capacitor

with decreasing electrode separation but attributed the effect to the changing electrical gradient. A large number of tests made during the course of this work have shown that the power-factor differences of air capacitors are independent of the voltages applied to the capacitors. In figure 13 are shown the observed power-factor differences of the three-terminal rotating-electrode capacitor and a fixed guard-ring capacitor over a wide range of voltages. Both the low- and high-

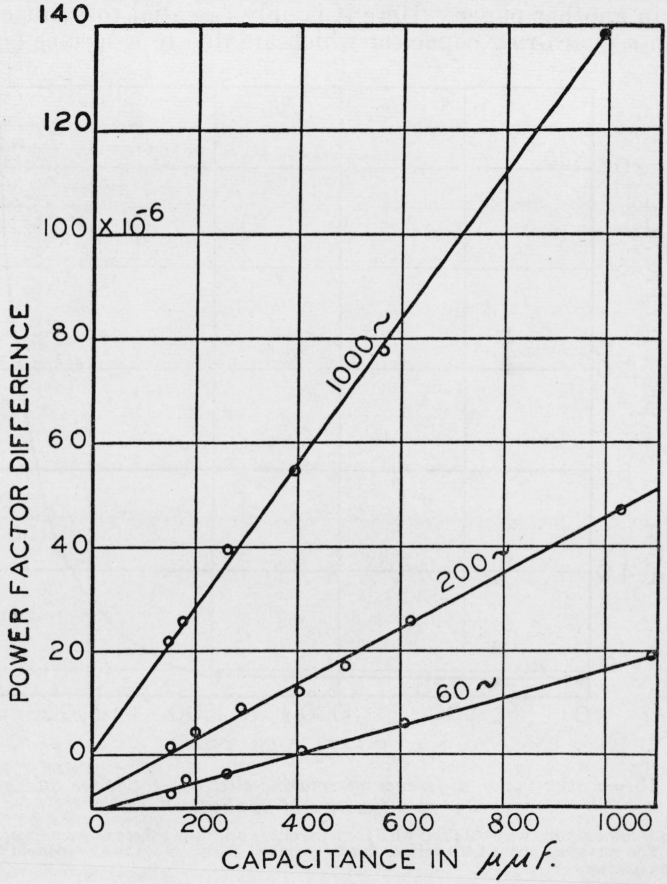

FIGURE 12.—*Variation in power factor with capacitance of the guard-ring capacitor.*

Power factor of the rotating-electrode capacitor at 150 $\mu\mu f$ is used as a reference.

voltage bridges were used to cover the voltage range indicated. No change in the measured values was observed between 10 volts and over 1,000 volts. At about 1,500 volts the gradient at the edges of the electrodes in the rotating-electrode capacitor became sufficient for corona formation and from this point the variation with voltage is rapid. It is evident from this curve that the power factor, below the corona point, is independent of the gradient, so that a power-factor increase, such as is shown in figure 12, must be a true function of the electrode separation.

Since the power factor of the guard-ring capacitor is a function of the electrode separation, it is reasonable to ascribe the losses to a surface effect. Definite proof that the power factor is a function of some surface phenomenon has been obtained by changing the nature of the surface, either by cleaning, polishing, or actually changing the electrode material.

An extensive survey of the effect of various types of electrode surfaces on power factor has been made, and it is planned to publish these results in another paper. Here it is only essential to point out that losses in a guard-ring capacitor which are due to a surface layer can

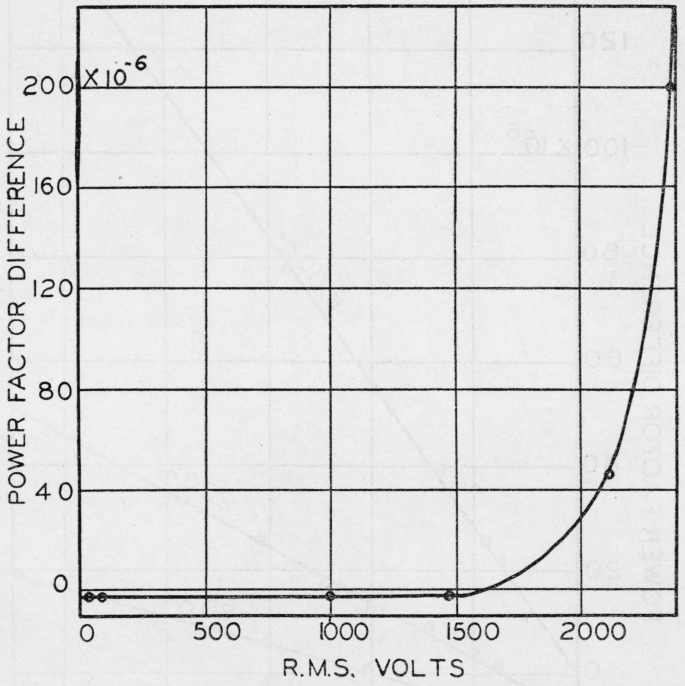

FIGURE 13.—*Power-factor difference of rotating-electrode capacitor and guard-ring capacitor as a function of applied voltage.*

The values below 500 volts were obtained with the low-voltage bridge and those above on the high-voltage bridge. The curvature above 1,500 volts is due to corona at the edges of the electrodes of the rotating electrode capacitor.

be represented, at a given frequency, by a resistance in series with the capacitor. Power factor due to such a cause will be linear with capacitance, and if a surface layer is the only cause of power loss, the losses will be proportional to the capacitance, thus permitting extrapolation to zero loss at zero capacitance. Applying this procedure to the data shown in figure 12, the intersections of the straight lines with the ordinate axis serve to define the true or absolute values of the power factors of the selected reference point at the frequencies indicated. Likewise, this intercept, when used as the zero point for the ordinate scale, will give actual power-factor values for the guard-ring capacitor. However, before this method of determining actual power factors can be considered reliable it is necessary to show that

there is no source of power loss in a guard-ring capacitor other than that which is proportional to the capacitance. A possible constant source would be the gas between the electrodes, but evacuation of this gas has shown its effect to be negligible. This is consistent with the computation of Kouwenhoven [1] that the conductivity of normally ionized air would give a power factor less than 1×10^{-8} at 60 cycles.

Other possible constant effects might be functions of the electrode area or the electrode material. Accordingly, four simple guard capacitors having areas different from that of the variable guard-ring capacitor were constructed of various electrode materials. Their electrode spacing was adjusted by means of small glass spacers

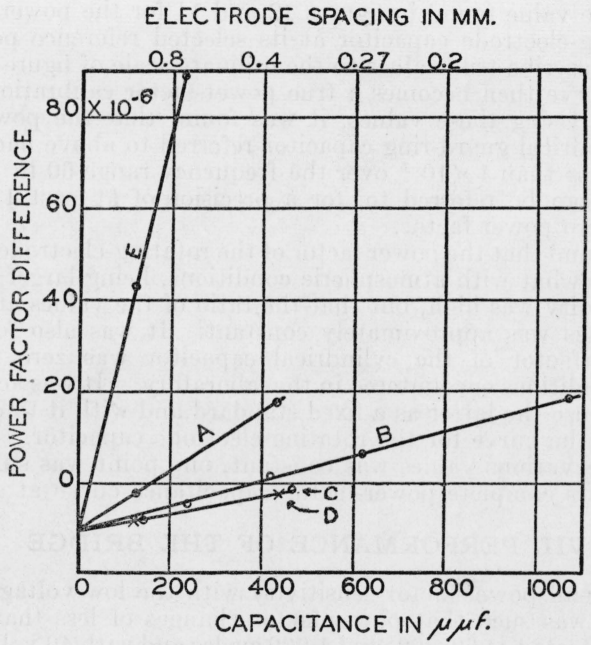

FIGURE 14.—*Variation in power factor with capacitance of guard-ring capacitors with various electrode materials.*

Power factor of rotating-electrode capacitor at 150 μμf used as a reference.

between the guard electrode and the high-potential electrode and their power factors at different spacings compared with those of the rotating electrode capacitor. The results of these observations at 60 cycles are illustrated in figure 14, where the values for the new capacitors are represented by *A*, *C*, *D*, and *E*, and *B* represents the set of points from figure 12 for the variable guard-ring capacitor at this frequency. The common intercept on the vertical axis indicates that the same value for the power factor of the variable standard at its selected reference point is obtained by comparison with each of five different guard-ring capacitors. Similar curves, with common intercepts, have also been obtained at 200 and 1,000 cycles. This agreement, together with the independence of energy losses on gas pressure, indicates that the power factor of a guard-ring capacitor is truly proportional to its capacitance. Consequently, a determination of the

rate of power-factor change with capacitance and an extrapolation to zero capacitance provides a method for determining the true power factor of a guard-ring capacitor.

It should be pointed out that the type of power-factor variation shown in figure 11 is believed to result from losses produced by a nonhomogeneous field. In the rotating-electrode capacitor there is an appreciable nonuniform field at the edges of the electrodes, and the relative effect of this nonuniformity decreases as the electrodes are interleaved. Consequently, if the observed losses are a function of the nonhomogeneous field, they will decrease with increasing capacitance. Such an effect would not be observed in a guard-ring capacitor in which the field is quite uniform.

Using the value found in figures 12 and 14 for the power factor of the rotating-electrode capacitor at its selected reference point, it is possible to ascribe true values to the ordinate scale of figure 11. The adjusted curve then becomes a true power-factor calibration for this capacitor. Using these values, it was found that the power factor of the cylindrical guard-ring capacitor referred to above had a power factor of less than 1×10^{-6} over the frequency range 60 to 1,000 c/s. This then can be referred to, for a precision of at least 1×10^{-6}, as having a zero power factor.

It was found that the power factor of the rotating-electrode standard varied somewhat with atmospheric conditions, being larger when the room humidity was high, but that the ratio of the values at different scale settings was approximately constant. It was also found that the power factor of the cylindrical capacitor was zero under all weather conditions encountered in the laboratory. It was accordingly possible to use the latter as a fixed standard and with it to determine a point on the curve for the rotating-electrode capacitor. Since the ratio of the various values was constant, one point was sufficient to determine its complete power-factor–capacitance curve at any given time.

VII. PERFORMANCE OF THE BRIDGE

The over-all power-factor sensitivity with the low-voltage form of the bridge was such that power-factor changes of less than 5×10^{-7} could be detected at 60, 200, and 1,000 cycles and with 40 volts applied to the bridge. Higher voltages resulted in no greatly increased sensitivity because of the instability produced in the ratio arm resistors with the greater heating effects. With the high-voltage bridge and 1,000 volts applied, a similar sensitivity was observed.

Although it is relatively simple to establish the sensitivity of the bridge, the degree of accuracy can be determined only by inference. If it is possible to obtain the same result, when factors likely to produce systematic errors are varied, then the accuracy is probably the same as the sensitivity. The data of figure 13, in which the values below 500 volts were obtained in the low-voltage bridge and those above in the high-voltage bridge, show a power-factor agreement to better than 5×10^{-7} between the two forms of the bridge. These data were taken at 60 c/s. Consistent results have also been obtained under a range of adjustments within the low-voltage form of the bridge. In table 1 are listed power-factor differences between the three-terminal rotating-electrode capacitor and the cylindrical guard-ring capacitor obtained with different ratio resistors, different balance procedures,

various ground impedances, and changing wave form. As pointed out before, the power factor of the cylindrical capacitor was found to be zero, so that the differences give directly the value for the rotating-electrode standard. Since the phase-defect angle of this capacitor was a function of humidity, a gentle stream of dry air was blown through the capacitor (at the guard-plate lead inlet 14 in fig. 9) in order to keep the relative humidity at a constant value throughout the tests summarized in the table. The data listed under "indirect balance" were obtained by balancing to ground each detector terminal of the bridge proper. The data under "direct balance" refer to direct balance of the bridge proper with the Y_{30} and Y_{40} admittances also balanced. The actual C_3 and C_3' values are listed to show that residuals may affect the separate balances of the bridge but not the differences obtained through the reversal procedure. Upon changing the balance procedure, the actual balance values were appreciably affected only at 60 cycles. This is to be expected because of the possible difference in the inductive effect in the detector leads in the presence of a large 60-cycle stray field. The result, however, changes in no case by more than 3×10^{-7}. Also shown are the effects of increasing admittance Y_{30} by adding capacitance between the detector terminal and ground and of adding a harmonic component in the voltage applied to the bridge. Here also the result is not definitely affected.

TABLE 1.—*Power-factor (phase-defect angle) values obtained in variable low-voltage bridge*

$$2(\phi_1-\phi_2)=\omega R_3(C_3-C_3')$$

ϕ_1=phase-defect angle in microradians of the three-terminal, rotating-electrode capacitor.
ϕ_2=0, representing the cylindrical guard-ring capacitor.

Frequency	R_3	By indirect balance			By direct balance		
		C_3	C_3'	ϕ_1	C_3	C_3'	ϕ_1
Cycles	*Ohms*	*μμf*	*μμf*	*Microradians*	*μμf*	*μμf*	*Microradians*
60	1,000	77.5	59.0	3.5	71.8	52.0	3.7
60	10,000	56.7	54.7	3.8	56.3	54.4	3.6
60	10,000	[1] 56.8	[1] 54.8	[1] 3.8			
200	1,000	57.8	53.0	3.0	57.8	53.1	2.9
200	10,000	54.95	54.45	3.1			
200	10,000	[1] 54.90	[1] 54.42	[1] 3.0	54.95	54.46	3.1
1,000	1,000	56.3	55.6	2.2	56.3	55.7	1.9
[2] 1,000	1,000	55.7	55.1	1.9	55.7	55.1	1.9
1,000	10,000	54.64	54.58	1.9	54.67	54.61	1.9
1,000	10,000	[1] 54.64	[1] 54.58	[1] 1.9			

[1] 2,500 μμf added between high-impedance detector terminal and ground.
[2] About 2-percent second harmonic introduced in applied voltage.

It is possible to provide a further check on the accuracy of the bridge by comparing the measured increase of the power factor of a capacitor when a resistor is placed in series with it, with the computed increase in power factor. The computed increase requires an evaluation of earth-capacitance effects which were not considered in the section on bridge theory. That this is necessary may be seen by referring to figure 15, which shows a resistor, r_1, in series with a capacitor, K_2. Quantities K_1 and r_2 represent impurities in r_1 and K_2,

respectively. There will also be present leakage and capacitance to ground from the junction 2 of r_1 and K_2. The increase in the power factor of K_2 due to r_1 may be measured in the bridge by connecting the terminals 1 and 3 to two of the bridge terminals. Since ground admittances from the bridge terminals only were considered in the bridge theory, it will be necessary to eliminate terminal 2 by transforming the star-shaped network of figure 15 into its equivalent delta-shaped network. The result of this transformation will be to give an effective admittance between terminals 1 and 3, which is modified by ground admittances K_3 and r_3. If C and R represent the equivalent parallel capacitance and resistance between terminals 1 and 3, they will be related to the actual values, upon the elimination of terminal 2, as follows:

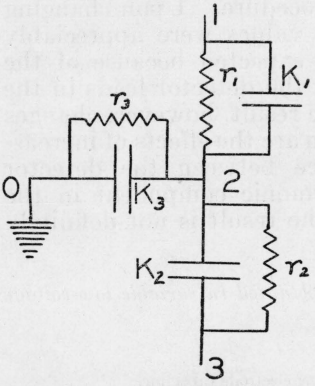

FIGURE 15.—*Arrangement of admittances after introducing a resistor in series with a capacitor.*

$$\frac{1}{R}+j\omega C=\frac{\left(\frac{1}{r_1}+j\omega K_1\right)\left(\frac{1}{r_2}+j\omega K_2\right)}{\frac{1}{r_1}+\frac{1}{r_2}+\frac{1}{r_3}+j\omega(K_1+K_2+K_3)}$$

If K_1 and K_3 are of the same order of magnitude as, or smaller than K_2, and if, in addition r_1 is sufficiently small that $r_1 \ll r_2$, $r_1 \ll r_3$, and $1 \gg \omega^2 r_1^2 K_2^2$, the above equation may be greatly simplified. Making the indicated approximations it is found that

$$C=K_2 \text{ and } \frac{1}{\omega RC}=\frac{1}{\omega r_2 K_2}+\omega r_1(K_2+K_3). \quad (35)$$

The last equation gives the equivalent power factor between terminals 1 and 3 and is the value which will be measured by the bridge. It is composed of two terms, the first representing the normal power factor of K_2 and the second the increase due to the addition of r_1 in the circuit. The presence of K_3 in the equation serves to illustrate a point mentioned in the first part of this paper, namely, that ground admittances must be evaluated when a capacitor and resistor are connected in series in any bridge arm. In this case K_3, the capacitance to ground, can be evaluated when r_1 is inserted between the power terminal and the rotating-electrode capacitor by taking the difference between the capacitance, first, when connected as a two-electrode instrument (1, 2, and 10 connected together, fig. 9) and then as a three-electrode capacitor.

The power-factor changes observed by inserting series resistors are listed in table 2, together with the values computed by the above equation. Small resistors having d–c values of 25, 111, and 798 ohms were used in the tests. The value of K_1+K_2 was 188 $\mu\mu$f.

TABLE 2.—*Observed and computed power-factor changes with resistors in series with capacitor*

Frequency	Series resistance	Computed value	Observed value	R_3
Cycles	*Ohms*	*Microradians*	*Microradians*	*Ohms*
60	798	56.6	56.7	10,000
60	111	7.9	8.1	10,000
60	111	----------	8.0	1,000
200	111	26.2	26.1	10,000
200	111	----------	26.4	1,000
1,000	111	131	130.2	1,000
200	25	5.9	6.0	1,000
1,000	25	29.5	29.5	1,000

In all but one case the agreement between observed and computed values is within 3×10^{-7}. Concerning the one exception, the 1,000-cycle value for the 111-ohm resistor, where the difference is 8×10^{-7}, it is believed that the discrepancy was in the d-c value of the resistance. A small inexpensive cathode-biasing resistor was used to permit easy shielding and it is probable that its a-c and d-c values are not identical within 1 percent.

From these tests it seems safe to draw the conclusion that the accuracy of the bridge for small power-factor measurements is of the order of the sensitivity, namely, $\pm5\times10^{-7}$.

VIII. SUMMARY AND CONCLUSIONS

1. The Schering-type bridge in either the original high-voltage orientation or in the conjugate arrangement offered the best means of measuring small differences in the power factors of two capacitors.

2. In a perfectly balanced bridge, with a Wagner ground connection, the balance condition involves only the effective admittances of the bridge proper (eq 6).

3. Errors due to an imperfect balance may be evaluated by eq 17. Such errors may be reduced by taking a second balance with the connections to two similar arms of the bridge interchanged (eq 20). Such an interchange also eliminates the necessity of evaluating the phase angles of resistance coils for power-factor determinations (eq 26).

4. The effect of imperfections in the balance of a Wagner grounding device can be materially reduced by adjustment of the admittances between the detector terminals and ground (eq 17a).

5. A bridge and detector system by which power-factor differences as small as 3×10^{-7} may be observed has been constructed. Such sensitivity has been obtained over the frequency range of 60 to 1,000 c/s and over a voltage range of 20 to 1,500 volts. The performance of the bridge is consistent over a wide range of operating conditions.

6. Air capacitors of conventional design could not be used as standards of power factor for values below 1×10^{-4} in the commercial- and audio-frequency range because of the losses in the solid insulation. A rotating-plate capacitor having three electrodes in order to eliminate the effect of solid insulation has been built and found satisfactory as a working standard for power-factor values down to 1×10^{-6}, even though its power factor is neither negligible nor constant with capacitance.

7. The power factors of guard-ring capacitors with electrode spacings of a few millimeters or less may be appreciably greater than 1×10^{-6}. In general, these power factors increase with decreasing electrode separation.

8. True power-factor values may be obtained from a determination of the rate of change of power factor in a guard-ring capacitor of variable electrode separation. The power-factor change has been found to be proportional to the capacitance, thus permitting an extrapolation to zero power factor at zero capacitance or infinite electrode separation. From this point of zero power factor the assignments of absolute values can be made to the differences in power factors as measured in the bridge. It is thus possible to determine the actual power factors of a variable capacitor throughout its range and then to use it as a calibrated standard for power-factor measurements.

It is a pleasure to acknowledge the financial support of the Utilities Research Commission of Illinois during part of the work and the cooperation of G. W. Gardiner, Jr., former research associate for the URC, who is now at New Mexico State College.

IX. REFERENCES

[1] W. B. Kouwenhoven and C. L. Lemmon, Trans. Am. Inst. Elec. Engrs. **49,** 952 (1930).
[2] Kazukeyo Ogawa, Researches Electrotech. Lab. Tokyo, No. 254 (1929); No. 277 (1930).
[3] J. C. Balsbaugh and Alfred Herzenberg, J. Frank. Inst. **218,** 49 (1934).
[4] W. B. Kouwenhoven and A. Baños, Trans. Am. Inst. Elec. Engrs. **51,** 202 (1933).
[5] H. Schering, Z. Instrumentenk. **40,** 120 (1920).
[6] Proc. Am. Soc. Testing Materials, pt. 1, 969 (1936) (D 150–36 T).
[7] D. W. Dye and T. Iowerth Jones, J. Inst. Elec. Engrs. (London) **72,** 169 (1933).
[8] K. W. Wagner, Elektrotech. Z. **32,** 1001 (1911).
[9] S. M. Goodhue, J. Frank. Inst. **217,** 87 (1934).
[10] J. G. Ferguson and B. W. Bartlett, Bell System Tech. J. **7,** 420 (1928).
[11] B. Hague, A. C. Bridge Methods, page 204 (Pitman Publishing Corporation, New York, N. Y., 1923).
[12] H. L. Curtis and F. W. Grover, Bul. BS **8,** 495 (1912) S177.
[13] C. N. Hickman, J. Opt. Soc. and Rev. Sci. Instr. **6,** 848 (1922).
[14] E. B. Rosa and N. E. Dorsey, Bul. BS **3,** 433 (1907) S65.

WASHINGTON, July 2, 1938.